CHAPTER 1
INTRODUCTION

What defines the quantum nature of a system? Is it particle size? The presence of the Planck constant? That the system is probabilistic rather than deterministic? While these may contribute to the quantum nature of a system, one of the hallmarks of a quantum system is in the indistinguishability of particles. Indistinguishability, also called indiscernible or identical particles, is the consideration that one particle can not be distinguished from another. While it is not the only hallmark of a quantum system, indiscernibility is a purely quantum phenomenon and can be used to determine the nature of a system.

While the concept seems simple, it has profound effects, particularly in quantum optics. But before we get there, let us further elaborate on the concept of indistinguishability. In classical mechanics, while two particles may be identical in their inherent qualities, we are still able to identify one from another using their relative positions and momenta. In addition to this, we are able to follow the subsequent trajectories and interactions of these particles. However, suppose we considered two electrons instead? What would the evolution of their collision look like?
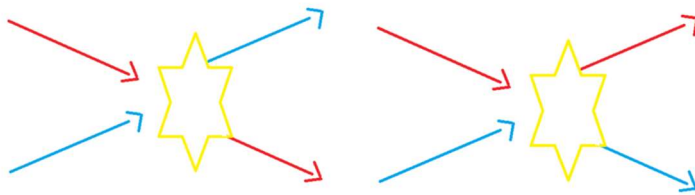

Figure 1 - Which Trajectory Do We Pick?

For two particles that are inherently not different from one another, which path seems more correct? Especially when taking Heisenberg's uncertainty principle into consideration, a particle's location ends up having very little meaning outside of the time of measurement. We now have no tangible way to distinguish the particles, and as such, we cannot follow particle trajectory in the same way as in the classical case.

What we have above seems rather abstract. How could this possibly have any real-life applications? However, as mentioned above, the lack of indistinguishability can lead to some remarkably interesting physical results. This leads us to the work done by Legero, Wilk, Kuhn, and Rempe. In 2003, they produced a paper detailing the mathematical framework that could demonstrate the distinguishability in photons. In particular, they found that if there was a difference in frequency between the photons, resulting in what they called the quantum beat.
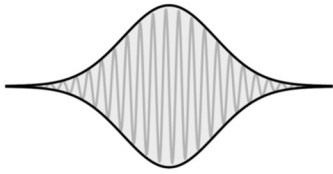

Figure 2 - The Beat Effect [12]

What is the quantum beat? Consider two photons that are distinguishable due to frequency. They also have a temporal delay with respect to one another, that is shorter than their wave packet length. Suppose they interact; the result is an interference effect that looks like a beat effect. This can be demonstrated experimentally by graphing coincidence counts of the output photons.

Coupled with this, one can determine how the frequency difference effects the presence of the Hong-Ou-Mandel (HOM) dip, the experimental signature of the HOM experiment. Provided that the beat is present, and there exists a change in the HOM dip, it can then be safely concluded that photon distinguishability is detectable through the HOM experiment.

It is my intention to convince the reader that the presence of a quantum beat and the change in the HOM dip can be used to determine the distinguishability of photon sources. First, we must calculate the second order correlation function, $g^{(2)}$ and graph it in hopes of detecting the quantum beat. This result is then integrated it over all possible detection times to find the probability distribution over all detections. This will be contrasted with the probability distribution of the HOM experiment. However, I'm getting a bit ahead of myself, before we get there, in Chapter 2, historical and mathematical context will be provided for the experiment and the analytic techniques used in this thesis. In Chapter 3, the techniques from the previous chapter are assembled to determine photon distinguishability, with a detailed analysis of the findings. Finally, in Chapter 4, I will draw conclusions with considerations for future experiments. It is my hope that you will have learned as much as I have through the reading of this thesis.

CHAPTER 2
CONTEXT

Before we can delve into the work done in this project, it is important that we have context for what we are doing. This includes historical and mathematical background for the work that contributed to this project. This is done in three parts:

1. The Framework of Quantum Information Processing and Quantum Optics
2. The Hong Ou Mandel Experiment
3. Hanbury-Brown Twiss Experiment

2.1   Quantum Background

One of the first things that needs to be established is the description of the object being tested, in this case, the photon. How does one quantify the photon? We address this question by first drawing parallels between the quantum harmonic oscillator and the quantization of the electromagnetic field. If this is indeed possible, we must then seek a form that allows information about frequency to be accessible to us, as that will be the main mode of distinguishability in this paper. With this, we will have then established the mathematical description of the object in question – the photon.

2.1.1   Quantum Information Processing

First proposed by Paul Benioff in 1980, and built upon by Feynman in 1981, quantum computation takes on the framework of quantum mechanics to perform simulations that are far beyond the ability of classical computation. In particular, it takes advantage of the principles of superposition and entanglement; both of which are fundamental to quantum mechanics. Let us first consider the superposition principle, and its use in quantum computation. Put simply, prior to measurement, a given quantum state is said to have access to and exists in multiple states.

Upon measurement, a state is picked with some probability, and no information of its previous state is accessible.

Before we continue in more depth, let us consider the basic premise behind classical computation. The basic unit in classical computation is the bit, which takes on either a value of 0 or 1. Given these bits, logic gates can be applied to them, which can serve to compare or combine the input bit values and provide an output bit.

In quantum computation, the basic unit of computation is the qubit. A qubit's information is encoded mathematically as follows:

$$|0\rangle = \begin{pmatrix} 1 \\ 0 \end{pmatrix}$$

$$|1\rangle = \begin{pmatrix} 0 \\ 1 \end{pmatrix}$$

This notation is called Dirac notation, and equations 2.1.1 and 2.1.2 denote the ground state and excited state, respectively. The qubit can exist as these states individually, or as a superposition of the two states. As mentioned, a superposition state exists as and has access to both the 0 and 1 states. A superposition is represented in Dirac notation as:

$$|\psi\rangle = \frac{1}{\sqrt{2}}(|0\rangle + |1\rangle)$$

Equation 2.1.3 is a normalised superposition of the ground and excited states. Each state has a complex coefficient (in this case $\frac{1}{\sqrt{2}}$), the modulus square of which would return the probabilities of measuring each state (which in this case would be $\frac{1}{2}$). Thus, upon repeated measurement of the system we would be able to attain outputs for both the ground and excited states with a probability of $\frac{1}{2}$. This elucidates the power of quantum computation over classical computation in its ability to produce all possible results over repeated iterations.

The second reason that quantum computation supersedes classical computation is due to entanglement. We have, thus far, only considered single qubits, but suppose we consider

multiple qubits instead. Like the single qubits, they exist as a superposition of basis states; however there exist states that can not be written as separable products of the individual states.

Consider a second qubit of the following form:

$$|\varphi\rangle = \frac{1}{\sqrt{2}}(|0\rangle - |1\rangle) \tag{2.1.4}$$

We can write a binary qubit state, mathematically, as the tensor product of the two states. This looks as follows:

$$|\varphi\rangle \otimes |\psi\rangle = \frac{1}{2}(|00\rangle + |01\rangle - |10\rangle - |11\rangle) \tag{2.1.5}$$

Equation 2.1.5 is a separable state, as it can be written as a product state of the two qubits. The state is spanned by four basis states, of which each qubit brings two basis states.

A non-separable state is one that can not be decomposed into a product of the two qubits. There exists some correlation term that can not be cleanly divided between the two qubits. When the state has this form, it is said to be an entangled state. The Bell states are examples of non-separable states, and they represent all combinations of maximally entangled basis vectors. They are:

$$|\Phi^+\rangle = \frac{1}{\sqrt{2}}(|00\rangle + |11\rangle) \tag{2.1.6}$$

$$|\Phi^-\rangle = \frac{1}{\sqrt{2}}(|00\rangle - |11\rangle) \tag{2.1.7}$$

$$|\psi^+\rangle = \frac{1}{\sqrt{2}}(|01\rangle + |10\rangle) \tag{2.1.8}$$

$$|\psi^-\rangle = \frac{1}{\sqrt{2}}(|01\rangle - |10\rangle) \tag{2.1.9}$$

2.1.2   States and Measurement

I have loosely used the terms measurement and state in section 2.1.1 but have yet to provide context for either. Here in this section, I hope to give enough context to paint an image of what they mean in terms of this thesis.

2.1.2.1   Object Property Representation

Suppose we were to consider an electron. What makes an electron an electron? What do we seek to know about it? Well, we can consider the electrons properties, such as mass, angular momentum, spin, etc. These properties give us information about the state of an object.

Mathematically, the set of all possible states within a property, is contained by a vector space called the Hilbert space. As an example, the set of all spin states of an electron spans a Hilbert space that is two-dimensional. This space has a set of vectors, called basis vectors, which span the entirety of the Hilbert space. As per the spin example, these basis vectors are the up and down spin states. One can generate any state in this Hilbert space as a linear combination of these basis states. Thus, a specific electron spin state is a vector within this Hilbert space, and as such, can be written as a linear combination of the up and down spin states.

In Dirac notation, these vector states are represented as 'kets.' Using our spin example again, the spin down state looks as follows:

$$|{\downarrow}\rangle = \begin{pmatrix} 1 \\ 0 \end{pmatrix}$$

We can see that equation 2.1.10 also has a column vector form that can be transposed into row vectors. These row vectors belong to a corresponding space that is dual to the Hilbert space. These dual vectors are a set of functions that act upon our vectors and produce scalars. This is represented in Dirac notation via 'bras,' which look as follows:

$$\langle{\downarrow}| = \begin{pmatrix} 1 & 0 \end{pmatrix}$$

Equation 2.1.11 in the bra corresponding to equation 2.1.10. A small, but important, note is to remember that the Hilbert space is a complex vector space, as such dual vectors are conjugate transposes of the vectors, rather than just the transposes.

2.1.2.2 Accessing these Properties

Now that we know what states are, and how they represent properties of an object; the next question is: how are we supposed extract this information? Much like in the classical world, information is gained via measurement. The act of measurement is represented mathematically via an operator. Each basis vector in the Hilbert space is an eigenvector that has an associated eigenvalue. When an operator acts upon these vectors, it pulls out the associated eigenvalue. Again, using the spin analogy, suppose we wanted to measure the spin in the z direction:

$$\langle \downarrow \, |S_z| \downarrow \rangle = \frac{\hbar}{2}\langle \downarrow \, | \downarrow \rangle = -\frac{\hbar}{2}$$

<div align="right">(2.1.12)</div>

The operator acts on the ket to pull out the appropriate eigenvalue, $-\frac{\hbar}{2}$. The set of all basis vectors form an orthonormal set, and when taking their inner product, we end up with a 0 if they are different, and a 1 if they are the same. In equation 2.1.12 they are the same and thus we are left with our measurement: $-\frac{\hbar}{2}$

In a superposition this will pull out a weighted average. Suppose we have some state $|\psi\rangle$, which looks as follows:

$$|\psi\rangle = \frac{1}{\sqrt{2}}(|\downarrow\rangle + |\uparrow\rangle)$$

<div align="right">(2.1.13)</div>

Then taking the same measurement of the spin as in equation 2.1.12, gives us:

$$\langle \psi |S_z| \psi \rangle = 0$$

<div align="right">(2.1.14)</div>

This measurement is also called the expectation value of the system. Often the averages of a given operator are denoted as $\langle \hat{A} \rangle$, wherein $\hat{A}$ is the operator in question.

2.1.3 Quantum Harmonic Oscillator

I have used the ground and excited states quite liberally in the section 2.1.1; however, I have not defined the framework from which they come from. Much like in classical computation, quantum computation also utilises a two-level system. One way this occurs is by piggybacking off of the solutions for the quantum harmonic oscillator. We define this problem as follows:
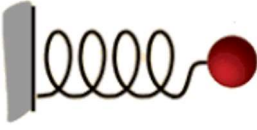
Consider a typical problem in classical mechanics: a particle oscillating on a spring. We know that this has the following Hamiltonian:

Figure 3 - Particle on a Spring [9]

$$H = \frac{p^2}{2m} - \frac{m\omega^2 x^2}{2} \tag{2.1.15}$$

Wherein:

- p is the particle momentum
- m is the particle mass
- x is the particle position
- And ω is the particle oscillation frequency

In order to make equation 2.1.15 a 'quantum' harmonic oscillator, the variables must be quantized. For the purposes of this paper, this will seem as though I'm simply putting hats on the variables while holding the canonical commutation relationship $[\hat{x},\hat{p}]=i\hbar$ in mind. However, the mathematics is far more in depth and beyond the scope of this paper.

$$\hat{H} = \frac{\hat{p}^2}{2m} - \frac{m\omega^2 \hat{x}^2}{2} \tag{2.1.16}$$

$$\hat{H}|\psi\rangle = E|\psi\rangle \tag{2.1.17}$$

The typical approach is to solve the Schrödinger equation, equation 2.1.17, which is a second order ordinary differential equation. This yields the following wavefunction:

$$\psi_n(x) = \frac{1}{\sqrt{2^n n!}} \sqrt[4]{\frac{m\omega}{\pi\hbar}} \, e^{-\frac{m\omega x^2}{2\hbar}} H_n\left(\sqrt{\frac{m\omega x}{\hbar}}\right) \qquad (2.1.18)$$

Wherein:

- H_n is the Hermite Polynomial, which is defined as follows:

$$H_n(x) = (-1)^n e^{z^2} \frac{d^n}{dz^n}(e^{-z^2}) \qquad (2.1.19)$$

- n defines the energy levels of the system

However, this is not quite what we're looking for. In order to get a more suggestive form, we can consider a small redefinition of the variables, which was first conceived by Paul Dirac:

$$\hat{a} = \sqrt{\frac{m\omega}{2\hbar}}\left(\hat{x} + \frac{i\hat{p}}{m\omega}\right) \qquad (2.1.20)$$

$$\hat{a}^\dagger = \sqrt{\frac{m\omega}{2\hbar}}\left(\hat{x} - \frac{i\hat{p}}{m\omega}\right) \qquad (2.1.21)$$

Equations 2.1.19 and 2.1.20 are called ladder operators and represent the action of lower or raising the energy level or the state. As an example, $\hat{a}^\dagger$, the creation/raising operator can act on the ground state to given us the first excited state:

$$\hat{a}^\dagger|0\rangle = |1\rangle \qquad (2.1.22)$$

Similarly, $\hat{a}$, the annihilation/lowering operator can take this excited state and lower it as follows:

$$\hat{a}|1\rangle = |0\rangle \qquad (2.1.23)$$

One can take equations 2.1.19 and 2.1.20 and rewrite the Hamiltonian as follows:

$$\hat{H} = \hbar\omega\left(\hat{a}^\dagger\hat{a} + \frac{1}{2}\right) \qquad (2.1.24)$$

Wherein the product of the ladder operators can be recast as $\hat{N}$, the number operator. This operator counts the number of excitations. For example, if the number operator were to act on the first excited state, it would count a single excitation:

$$\hat{N}|1\rangle = 1$$

We have now established the general idea behind the quantum harmonic oscillator. However this framework can not be used as is, there needs to be a way to relate it directly to the creation of photons. How can this be done? This is addressed in the next section.

2.1.4 Quantum Optics

Of the multiple proposed modes for computation, one of the first and most popular is the photon. Information can be encoded into the photon in multiple modes: frequency, spatial, polarization, and time of arrival. This is a natural choice for candidacy due to the photon's high durability (weak interactions with the environment) and high mobility. In this thesis, we will pay particular attention to the frequency mode of encoding. The harmonic oscillator framework is a natural fit for describing photon interactions such as excitation, absorption, and photon counting, and will be demonstrated as such going forward.

2.1.4.1 Quantization of an Electromagnetic Field

We can not employ the harmonic oscillator convention as is. First, it must be shown that this framework is indeed a natural fit for the photon. To do this, first consider the classical electromagnetic fields governed by Maxwell equations (in a vacuum):

$$\vec{\nabla} \cdot \vec{E} = 0$$

$$\vec{\nabla} \cdot \vec{B} = 0$$

$$\vec{\nabla} \times \vec{E} = -\frac{\partial B}{\partial t}$$

$$\vec{\nabla} \times \vec{B} = -\frac{1}{c^2}\frac{\partial E}{\partial t}$$

Wherein:

- $\vec{\nabla}$ is the nabla/del operator
- $\vec{E}$ is the electric field

- $\vec{B}$ is the magnetic field

- c is the speed of light within a vacuum

We can take the curl of equations 2.1.27 and 2.1.28, and when we do we find the following second order differential equations:

$$\vec{\nabla}^2\vec{E} = \frac{1}{c^2}\frac{\partial^2 E}{\partial t^2} \tag{2.1.30}$$

$$\vec{\nabla}^2\vec{B} = \frac{1}{c^2}\frac{\partial^2 B}{\partial t^2} \tag{2.1.31}$$

The solutions for the electric field have the following form, (Majidy, Laflamme, & Wilson, 2021):

$$\vec{E}(\vec{r},t) = \sum_{k,\lambda} \sqrt{\frac{\hbar\omega_k}{2}}\left(ia_{k,\lambda}\vec{u}_{k,\lambda}(\vec{r})e^{-i\omega_k t} - ia^*{}_{k,\lambda}\overrightarrow{u^*}_{k,\lambda}(\vec{r})e^{i\omega_k t}\right) \tag{2.2.32}$$

Wherein:

- $\vec{r}$ is a vector that denotes an arbitrary direction

- $\vec{k}$ is the wave vector in the direction of wave propagation

- λ denotes the polarization of the vector, perpendicular the direction of propagation

- ω_k is the frequency of the wave, such that

$$\omega_k = \frac{k}{c} \tag{2.1.33}$$

- $\vec{u}_{k,\lambda}(\vec{r})$ are spatial plane wave solutions of the form (also called mode functions):

$$\vec{u}_{k,\lambda}(\vec{r}) = \frac{\vec{E}(\lambda)}{\sqrt{V}}e^{i(\vec{k}\cdot\vec{r})} \tag{2.1.34}$$

   - With $\vec{E}(\lambda)$ representing the electric field component with respect to polarization
   - V representing the unit volume within which the field is confined
- $a_{k,\lambda}$ and $a^*{}_{k,\lambda}$ representing the complex amplitudes associated to each temporal mode

Equation 2.1.31 is found with the assumption that the wave is propagating in a vacuum, and, as such, there are no free charges. This implies that the polarization is orthogonal to the direction propagation.

Now to consider the magnetic field, which can be found using equation 2.1.31, (Majidy, Laflamme, & Wilson, 2021)

$$\vec{B}(\vec{r},t) = \sum_{k,\lambda} \sqrt{\frac{\hbar\omega_k}{2}} (ia_{k,\lambda} \vec{v}_{k,\lambda}(\vec{r})e^{-i\omega_k t} - ia^*_{k,\lambda}\vec{v^*}_{k,\lambda}(\vec{r})e^{i\omega_k t}) \tag{2.1.35}$$

Wherein:

- $\vec{v}_{k,\lambda}(\vec{r})$ are spatial plane wave solutions of the form (also called mode functions):

$$\vec{v}_{k,\lambda}(\vec{r}) = \frac{\vec{B}(\lambda)}{\sqrt{V}} e^{i(\vec{k}\cdot\vec{r})} \tag{2.1.36}$$

  o With $\vec{B}(\lambda)$ representing the magnetic field component with respect to polarization and given by the following relationship:

$$\vec{B}(\lambda) = k \times \vec{E}(\lambda) \tag{2.1.37}$$

Given the electric and magnetic field equations defined above, we can now determine the energy of the electromagnetic field as follows:

$$H = \frac{1}{2} \int_V d\vec{r}\, \vec{E}^2 + c^2\vec{B}^2 \tag{2.1.38}$$

$$H = \frac{1}{2} \sum_{k,\lambda} \hbar\omega_k (a^*_{k,\lambda}a_{k,\lambda} + a_{k,\lambda}a^*_{k,\lambda}) \tag{2.1.39}$$

Equation 2.1.39 looks very close to quantum harmonic oscillator solutions, however there are some considerations before we can call them similar. As with the quantum harmonic oscillator, we must quantize the complex amplitudes. Again, this is more complex than what it seems (simply putting hats atop the operators and changing the star to a dagger); however, suffice it to understand that they are more complex than what is given. We must also consider that these operators obey bosonic commutation relations, i.e.:

$$[\hat{a}_{k,\lambda}, \hat{a}^{\dagger}{}_{k',\lambda'}] = \delta_{k,k'}\delta_{\lambda,\lambda'} = \begin{cases} 0 \; if \; k \neq k' \, and \; \lambda \neq \lambda' \\ 1 if \; k = k' \, and \; \lambda = \lambda' \end{cases} \qquad (2.1.40)$$

Our Hamiltonian then becomes:

$$\hat{H} = \frac{1}{2}\hbar\omega \sum_{k,\lambda} \left(\hat{a}^{\dagger}{}_{k,\lambda}\hat{a}_{k,\lambda} + \hat{a}_{k,\lambda}\hat{a}^{\dagger}{}_{k,\lambda}\right) \qquad (2.1.41)$$

$$\hat{H} = \hbar\omega \sum_{k,\lambda} \left(\hat{a}^{\dagger}{}_{k,\lambda}\hat{a}_{k,\lambda} + \frac{1}{2}\right) \qquad (2.1.42)$$

Which takes advantage of the equation 2.1.40 to get the equation 2.1.42. We can safely conclude that the photon indeed follows a harmonic oscillator framework, with the careful consideration that ladder operators follow a bosonic commutation relationship. However we have a final problem to address, equations 2.1.32 and 2.1.35 are with respect to spatio-polarization. How do we involve frequency encoding?

2.1.4.2   Temporal Mode Functions

In this thesis we pay particular consideration to the frequency mode of encoding. As such, we can not use the polarization mode functions found in section 2.1.4.2. Therefore, we need solutions associated to frequency instead. How do we go about this?

Mode functions were first characterized by Glauber and Titulær in 1965 and were proposed as a solution to the real-world problem that photon emissions are never exactly monochromatic, but instead a wave packet that holds multiple frequencies (Glauber & Titualær, 1966). They considered that the spectral width, the spectrum of frequencies contained by a photon, is roughly the inverse of the duration of the wave packet. This gave rise to the idea of a spatio-temporal wave packet. As time and frequency are Fourier transforms of one another, they were then able to characterize the wave packet with respect to its frequency as well. This derivation will be done entirely without Fourier transforms, and as such will not be defined further in this thesis. Suffice it to say that there is an intrinsic relationship between time and frequency that allows for this transformation to occur.

Much like equation 2.1.32, we will assume a similar general form for the equation of an electric field (in the frequency domain):

$$\vec{E}(\vec{r},t) = \int d\omega \sqrt{\frac{\hbar\omega_k}{2\epsilon_0}} [i\hat{a}(\omega) \ e^{-i\omega_k(t-\frac{z}{c})} - i\hat{a}^\dagger(\omega)e^{+i\omega_k(t-\frac{z}{c})}] \qquad (2.1.43)$$

We seek to create new creation and annihilation operators that will generate discrete photons which consist of a collection of frequencies. Thus, we define a linear superposition of these $\hat{a}(\omega)$ and $\hat{a}^\dagger(\omega)$ which are modified by a set of complete and orthogonal weight functions $f_j(\omega)$. This looks as follows:

$$\hat{A} = \int d\omega \ \hat{a} \ f_j{}^*(\omega) \qquad (2.1.44)$$

$$\hat{A}^\dagger = \int d\omega \ \hat{a}^\dagger \ f_j(\omega) \qquad (2.1.45)$$

These operators obey the bosonic commutation relationships:

$$[\hat{A}_k, \hat{A}^\dagger{}_{k\prime}] = \delta_{k,k\prime} \qquad (2.1.46)$$

As mentioned above, these orthogonal weight functions, $f_j(\omega)$, are also complete. This means that they obey the following relationship:

$$\sum_j f_j{}^*(\omega)f_j(\omega') = \delta(\omega - \omega') = 0 \qquad (2.1.47)$$

Using this, we can now define inverse relationships of the following form:

$$\hat{a}(\omega) = \sum_j \hat{A} f_j(\omega) \qquad (2.1.48)$$

$$\hat{a}^\dagger(\omega) = \sum_j \hat{A}^\dagger f_j{}^*(\omega) \qquad (2.1.49)$$

We now have all the ingredients to create our temporal mode functions. These are defined using equations (2.1.34, 2.1.39, and 2.1.40) as:

$$v_j(z,t) = i \int d\omega \sqrt{\frac{\hbar\omega_k}{2\epsilon_0}} f_j(\omega)e^{-i\omega_k(t-\frac{z}{c})} \qquad (2.1.50)$$

$$v_j^*(z,t) = -\int d\omega \sqrt{\frac{\hbar\omega_k}{2\epsilon_0}} \, i f_j^*(\omega) e^{+i\omega_k\left(t-\frac{z}{c}\right)} \tag{2.1.51}$$

These temporal mode functions are key to the set up of the quantum beat problem, as they play the role of defining the 'shape' of the photon. All future calculations will be done in units of $\hbar\omega_k$, or natural units for simplicity.

This thesis will use the temporal mode function for the Gaussian photon given by Legero, Kuhn, Wilk and Rempe (LKWR):

$$\zeta_{a(b)}(t) = \sqrt[4]{\frac{2}{\pi}} e^{-\frac{(t\pm\delta\tau)^2}{2} - i\left(\omega_0\pm\frac{\Delta}{2}\right)t} \tag{2.1.52}$$

Wherein:

- $\delta\tau$ represents the temporal offset between the pulses

  $+\frac{\delta\tau}{2}$ representing photon a

  o $-\frac{\delta\tau}{2}$ representing photon b

- Δ representing the difference between the frequencies
- Frequencies that are centered about ω_0

  o Thus $\omega_0 + \frac{\Delta}{2}$ representing photon a

  o And $\omega_0 - \frac{\Delta}{2}$ representing photon

The Gaussian mode functions defines an idealized wave packet. It is called a 'packet' as it consists of multiple wavenumbers clustered about a single value. This mathematically exemplifies ideal monochromatic emission. This concludes the development of a mathematical representation of a photon that contains frequency dependence.

$\sim$

We have successfully defined the Gaussian photon with respect to frequency under a quantum framework. We are now able to employ these photons for experimentation which will be elaborated upon in the next section – The Hong-Ou-Mandel (HOM) experiment.

2.2   Hong-Ou-Mandel Experiment

A landmark experiment in the field of quantum optics, the HOM effect was first demonstrated by Chung Ki Hong (홍정기), Zheyu Ou (区泽宇), and Leonard Mandel in 1987 at the University of Rochester. In this section we will dissect this experiment and put it under a mathematical framework that will make it accessible for our purposes. We will begin with the experimental set up with a follow up discussion on the results and analysis.

2.2.1   Experimental Set Up

Though this experiment is a hallmark in quantum optics, its execution is deceptively simple. It employs the use of a beam splitter upon which two photons are incident. The resultant photons detections are analysed for their temporal separation. But we are getting ahead of ourselves; let us break this down a little further, starting with the beam splitter.

The beam splitter is an optical device that is a cube of glass, consisting of two glass prisms. It takes any input beam and divides it into two 'arms.' In most experiments, a beam splitter splits the input beam into two constituent halves, and as such is called a $\frac{1}{2}$ beam splitter. However, there are other divisions of the input beam, such as the $\frac{1}{3}$ beam splitter, which divides the beam into $\frac{1}{3}$ and $\frac{2}{3}$ output arms.

As mentioned above, there are two photons, we call them photons a and b, that are incident upon the beam splitter. Theoretically there are four possible outcomes:

1. Photon a/b is reflected while photon b/a is transmitted (this has a multiplicity of 2) – as seen in figure 4, in the image labelled 1 and 4 respectively
2. Both input photons are transmitted – as seen in figure 4, in the image labelled 2
3. Both input photons are reflected – as seen in figure 4, in the image labelled 3
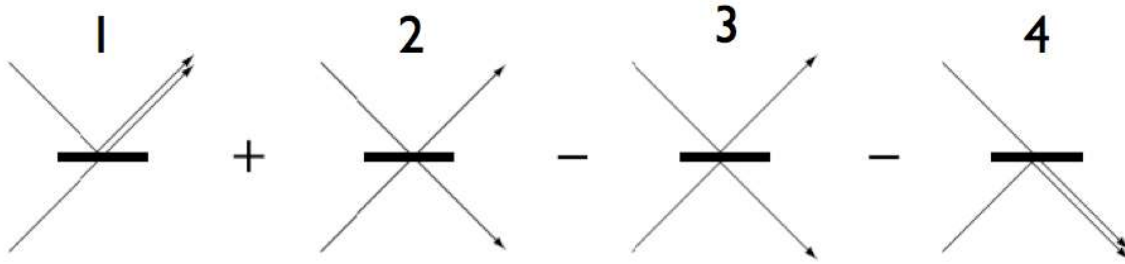

Figure 4 - The Possible Beam Splitter Outputs [5]

This can be represented mathematically by the application of photons' creation operators. This looks as follows:

$$\hat{a}^{\dagger}\hat{b}^{\dagger}|00\rangle_{ab}=|11\rangle_{ab}$$

<div align="right">(2.2.1)</div>

These input photons will go through a beam splitter. This can be modelled as a unitary operator and looks as follows:

$$\begin{pmatrix}\hat{a}^{\dagger}\\\hat{b}^{\dagger}\end{pmatrix}\begin{pmatrix}1 & 1\\1 & -1\end{pmatrix}=\begin{pmatrix}\hat{c}^{\dagger}\\\hat{d}^{\dagger}\end{pmatrix}$$

<div align="right">(2.2.2)</div>

Wherein:

- $\hat{a}^{\dagger}$ and $\hat{b}^{\dagger}$ are the creation operators of the photons incident upon the beam splitter
- $\hat{c}^{\dagger}$ and $\hat{d}^{\dagger}$ are the creation operators of the photons output from the beam splitter
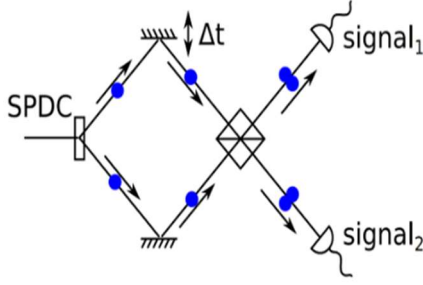
Figure 5 - Experimental Setup [11]

The output photons are measured via two photodetectors on the other output arm of the beam splitter. This can be seen in figure 5. As the output photons were incident upon the photodetectors, the researchers measured the coincidence counts, that is to say that they measured a count when one photon was detected in each photodetector, simultaneously.

2.2.2 Results

What they found went against their expectations in that when the photons had no temporal overlap and were completely indistinguishable, no coincidence was measurable. That is to say that both photons were incident upon one photodetector or the other. This can be seen graphically as the HOM dip. This is demonstrated, in figure 6.
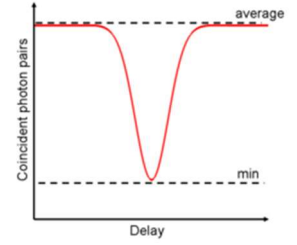

Figure 6 - The HOM Dip [6]

This result can be demonstrated mathematically by considering the transformation given in equation 2.2.2. We can rewrite the creation operators of photon a and b as a linear combination of the output creation operators of photons c and d. This looks as follows:

$$\hat{a}^\dagger = \frac{1}{\sqrt{2}}(\hat{c}^\dagger + \hat{d}^\dagger) \tag{2.2.3}$$

$$\hat{b}^\dagger = \frac{1}{\sqrt{2}}(\hat{c}^\dagger - \hat{d}^\dagger) \tag{2.2.4}$$

We can then rewrite equation 2.2.1 as follows:

$$\hat{a}^\dagger \hat{b}^\dagger |00\rangle_{ab} = \frac{1}{2}(\hat{c}^\dagger + \hat{d}^\dagger)(\hat{c}^\dagger - \hat{d}^\dagger)|00\rangle_{cd} \tag{2.2.5}$$

Operators from two different Hilbert spaces commute, thus $\hat{c}^\dagger \hat{d}^\dagger = \hat{d}^\dagger \hat{c}^\dagger$. As such we are left with:

$$\hat{a}^{\dagger}\hat{b}^{\dagger}|00\rangle_{ab}=\frac{1}{2}((\hat{c}^{\dagger})^{2}-(\hat{d}^{\dagger})^{2})|00\rangle_{cd} = \frac{1}{\sqrt{2}}(|20\rangle_{cd} - |02\rangle_{cd}) \qquad (2.2.6)$$

This gives us the exact result found in experiment, with no $|11\rangle_{cd}$ term to suggest a coincidence count.

~

We have now established the experimental framework that will be the basis for this thesis. In the last section, we will be discussing the technique used to analyze our results, the second-order correlation function.

2.3   Hanbury-Brown Twiss Experiment

Before we continue with quantum optics, we will take a brief foray into astronomy to the work of Robert Hanbury-Brown and Richard Q. Twiss. This will provide us with the last piece of the puzzle – the analytic method – that will help us understand the results that we generate.

2.3.1   Historical Context

The primary mode used for determining the diameter of stars was the Michelson interferometer. The general idea of this technique is to collect light, from a single source, upon two mirrors, which are separated by some distance. This light was then focussed upon the telescope and onto a focal plane. If the light was coherent, then an interference pattern would be formed. As the distance between the mirrors was changed, so too would the interference pattern. One could determine the angular size of the star in question, by studying the change in the fringe pattern relative to the distance between the mirrors.

This idea falls apart when the distance between the mirrors is too large, this can result in collection mirrors becoming extremely sensitive to outside noise and preventing any viable

measurements from being made. Cue Hanbury-Brown and Twiss (HBT), who proposed a simpler arrangement. They argued that the mirrors could be cut out of the equation altogether and simply focus the light directly onto a beam splitter. This prevented the issue of the mirrors being too sensitive to manage large separations.

HBT were met with vehement skepticism and criticism. As such, they demonstrated the validity of their idea with what is now known as the HBT experiment, which we will discuss further in this next section.

2.3.2 The Experiment and the Correlation Function

A proof of concept was developed to demonstrate the validity of the interferometer. Instead of light from a distant star, HBT used a mercury lamp, and had this light incident upon a half-silvered mirror. This served to split the incident beam into two constituent parts. Each output beam is then amplified by a photomultiplier to create a current that would be detectable by their equipment. An AC-coupled amplifier was used as well, which gave outputs proportional the fluctuations in current. One photocurrent was delayed by a time τ by passing it through a time delay generator. The two signals were then integrated and averaged over a given time period. HBT made the conclusion the resultant current is proportional to the input beam intensity; we can assume that current fluctuations will also be proportional to intensity fluctuations. Thus, we have that:

$$\langle \Delta i_1(t) \Delta i_2(t+\tau) \propto \langle \Delta I_1(t) \Delta I_2(t+\tau) \rangle$$

<div align="right">(2.3.1)</div>

We have the general idea of what the output should look like, but how does one mathematically demonstrate a fluctuation? This question brings us to the introduction second-order correlation function. This is given by the following equation (Fox, 2006):

$$g^2(t) = \frac{\langle I_1(t) I_2(t+\tau) \rangle}{\langle I_1(t) \rangle \langle I_2(t+\tau) \rangle}$$

<div align="right">(2.3.2)</div>

Equation 2.3.2 is indeed similar to the equation 2.3.1.

How does this relate to quantum optics? We do not have photocurrents, or intensities, but rather we have individual photons instead. As the number of photons increase, the more intense the light source becomes, thus we can draw a proportionality between the number of photons and intensity. This relationship lends itself to the following redefinition of $g^2(t)$ (Fox, 2006):

$$g^2(t) = \frac{\langle n_1(t)n_2(t+\tau)\rangle}{\langle n_1(t)\rangle\langle n_2(t+\tau)\rangle} \qquad (2.3.3)$$

With equation 2.3.3, we now have our final piece to the experimental puzzle, a way to understand our results from the HOM experiment in a quantifiable way.

~

With this last section, we have set up the experimental building blocks for this thesis. In section 2.1, a mathematical framework is established for the object being measured, the photon. Section 2.2 elaborates upon the experimental technique that the photons will be subject to. And finally, in section 2.3 outlines the technique used to quantify the results of the experiment. In the next chapter we will try to employ these blocks to build an experiment that will help determine the distinguishability of the photons emitted from a given source.

CHAPTER 3
METHODOLOGY AND RESULTS

In chapter 2 we established the historical context and mathematical framework behind the experiment and analysis for the question we seek to posit: Can we determine if two photons are distinguishable with the Hong-Ou-Mandel (HOM) experiment? In this chapter we employ what we have learned in chapter 3 to answer this question. Legero, Wilk, Kuhn, and Rempe (LWKR) demonstrated the quantum beat by graphing the two-photon coincidence probability against the detection time. In this thesis, the framework prescribed by Woolley, Lang, Eichler, Wallraff, and Blaise will be used to determine photon distinguishability (Woolley, Lang, Eichler, Wallraff, & Blais, 2013). First, we find the second-order correlation function and by graphing it, demonstrate the presence of the quantum beat. Second, we integrate the second order correlation function over all possible initial detection times and detection delay times. The result is a probability distribution that will be used to detect differences between the HOM dip and what we have found. Having established both the quantum beat and the change in the HOM dip, we can safely conclude whether or not the HOM experiment is a viable test for photon distinguishability.

3.1   The Second-Order Correlation Function – HOM Edition

We have, from equation 2.3.3, the second order correlation function. However, we are particularly interested in the correlations between the output photons, rather than the input. Thus, we amend $g^2(t)$ as follows:

$$g^2(t) = \frac{\langle \hat{N}_c(t)\hat{N}_d(t+\tau)\rangle}{\langle \hat{N}_c(t)\rangle\langle \hat{N}_d(t+\tau)\rangle} \tag{3.1.1}$$

We can recast equation 3.1.1, to a form that is more useful to us, as the products of the photons' respective creation and annihilation operators. With consideration to the subtlety that operators belonging to two different Hilbert spaces commute. As such, we have that $[\hat{c}^\dagger, \hat{d}^\dagger] = [\hat{c}^\dagger, \hat{d}] = 0$. We can then rewrite equation 3.1.1 in the normal ordering convention, such that the creation operators are written to the left and the annihilation operators are written to the right. This looks as follows:

$$g^2(t) = \frac{\langle \hat{c}^\dagger(t)\hat{d}^\dagger(t+\tau)\hat{c}(t)\hat{d}(t+\tau)\rangle}{\langle \hat{c}^\dagger(t)\hat{c}(t)\rangle\langle \hat{d}^\dagger(t+\tau)\hat{d}(t+\tau)\rangle}$$

<div align="right">(3.1.2)</div>

With equation 3.1.2 we are able to determine the correlations between the output photons; however, we have a problem: we do not know what these output photons look like. So how do we progress? Recall from chapter 2, equation 2.2.2, which outlines the transformation of the incident photons through the beam splitter into the emitted photons. While we may not know what photons c and d look like, we do know what incident photons a and b look like. Using equation 2.2.2, we can rewrite 3.2 with respect to the input photons a and b. The resulting equation has a total of sixteen terms; however, we can simplify this by making some considerations. The first is to recognize that we can ignore any terms that contain the square of the creation or annihilation operator, this is due to the consideration that we are only generating single photons. This eliminates twelve terms, leaving us with 4. The resultant function looks as follows:

$$g^2(t) = \frac{1}{4}\frac{\langle \hat{a}^\dagger(t)\hat{b}^\dagger(t+\tau)\hat{a}(t)\hat{b}(t+\tau) - \hat{a}^\dagger(t)\hat{b}^\dagger(t+\tau)\hat{b}(t)\hat{a}(t+\tau) - \hat{b}^\dagger(t)\hat{a}^\dagger(t+\tau)\hat{a}(t)(t)\hat{b}(t+\tau) + \hat{b}^\dagger(t)\hat{a}^\dagger(t+\tau)\hat{b}(t)\hat{a}(t+\tau)\rangle}{\langle \hat{a}^\dagger(t)\hat{a}(t) + \hat{b}^\dagger(t)\hat{b}(t) + \hat{b}^\dagger(t)\hat{a}(t) + \hat{a}^\dagger(t)\hat{b}(t)\rangle\langle \hat{a}^\dagger(t+\tau)\hat{a}(t+\tau) + \hat{b}^\dagger(t+\tau)\hat{b}(t+\tau) + \hat{b}^\dagger(t+\tau)\hat{a}(t+\tau) + \hat{a}^\dagger(t+\tau)\hat{b}(t+\tau)\rangle}$$

<div align="right">(3.1.3)</div>

Equation 3.1.3 still looks rather intimidating; and thus we make our second consideration: The actual form of these time dependent creation and annihilation operators. As we are dealing with photons, they are not simply the creation and annihilation operators, but are instead modified by scalar mode functions. In particular, we are dealing with temporal mode functions, which for now we will simply denote as $\zeta_{a(b)}(t)$. These mode functions, rather than operators, carry the time dependence of the system. As such, we are able to separate the time dependence from the operators to look as follows:

$$\hat{a}^\dagger(t) = \zeta_a(t)\hat{a}^\dagger$$

<div align="right">(3.1.4)</div>

Our third consideration: From equation 3.1.2, we can see that we are calculating expectation values. In order to calculate expectation values, one must specify the state that is measured. We have established an equation (equation 3.1.3) that is defined via the input photon modes, and as mentioned in chapter two, the HOM experiment begins with two photons, a and b, being produced from the vacuum state. Thus, our expectation values will be calculated with the state in which the input photons are produced:

$$|\psi\rangle = \hat{a}^\dagger \hat{b}^\dagger |00\rangle_{ab}$$

Our final consideration is for the denominator. As there will always be a photon output from the beam splitter, there will be an excitation in each output mode. As such, the expectation values of the number operators on this state will always evaluate to one.

When we combine the final three considerations, we end up with the following simplified expression:

$$g^2(t) = \frac{1}{4}|\zeta_a(t+\tau)\zeta_b(t) - \zeta_b(t+\tau)\zeta_a(t)|^2$$

Equation 3.1.6 is final form for $g^2(t)$ for the HOM experiment that will be used to calculate probability distributions for the Gaussian photon.

3.2   Probability Distribution and Detection of the Quantum Beat

Now that we have established the second order correlation function associated to the HOM experiment. In this section, we seek to use it for the Gaussian photon distribution. First, we will determine if $g^2(t)$ oscillates with respect to the detection time τ. Finding this relationship would suggest the presence of the quantum beat. We can confirm this by graphing the resulting function and seeing if there is a beat pattern as the difference in frequency is increased. However, this is only the first step. The $g^2(t)$, much like an expectation value, only gives us the average detection time. If we want to determine if a given detection time has a certain probability of occurrence, we must consider the entire distribution, not just the mean. In order to do this, we will integrate the second-order correlation function twice, once over all first photon detection times (t) and then over all possible detection time delays (τ). This gives a distribution of all possible photon measurements, and thus the likelihood of simultaneously detecting photons in both output photodetectors. We confirm this graphically by contrasting the resultant dip to the HOM dip. If there is a demonstrable difference, then we can reliably confirm that this experiment can be used as a test to determine the distinguishability of photons.

3.3 The Gaussian Photon

Let us consider a Gaussian photon, previously described in equation 2.1.51. This looks as follows:

$$\zeta_{a(b)}(t) = \sqrt[4]{\frac{2}{\pi}} e^{-\frac{(t\pm\delta\tau)^2}{2} - i\left(\omega_0 \pm \frac{\Delta}{2}\right)t}$$

(3.2.1)

The associated $g^2(t)$, is then:

$$g^2(t) = \frac{\cosh(2\tau\delta\tau) - \cos(\tau\Delta)}{\pi} e^{-(\delta\tau^2 + \tau^2) - 4t(t+\tau)}$$

(3.2.2)

This function can be graphed to see how the photons will interfere with one another. However, just looking at this function we can see that the function oscillates with respect to detection delay times τ, suggesting that we will see the quantum beat. Figure 7 demonstrates that over different frequency differences, $\Delta = 0, \frac{3}{2}\pi$ and 3π, we are able to detect the quantum beat.
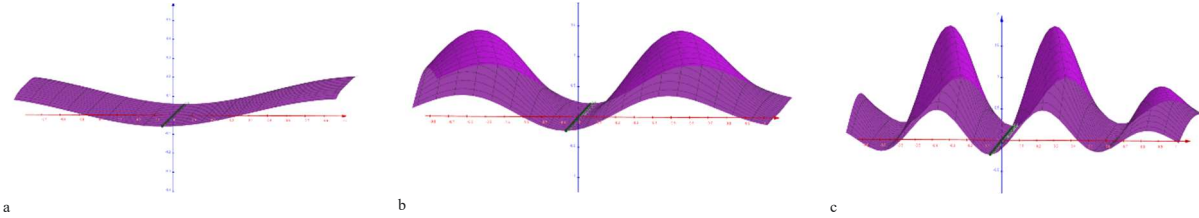

a   b   c

Figure 7 - Second Order Correlation Function - The blue axis represents the correlation between the output photons $g^2(t)$, the red axis representing the detection time difference τ and the green axis representing the temporal separation between photons $\delta\tau$ time for frequency difference of a) 0 b) $\frac{3}{2}\pi$ and c) 3π.

Now that we have confirmed presence of the quantum beat. Let us find the associated probability distribution by first integrating this over all first photon detection times (t).

$$\int dt \, g^2(t) = \frac{\cosh(2\tau\delta\tau) - \cos(\tau\Delta)}{2\sqrt{\pi}} e^{-(\delta\tau^2 + \tau^2)}$$

(3.2.3)

Notice that for non-zero detection time delay (i.e. $\tau \neq 0$), With the final probability distribution found when we integrate what we have above with the detection time delays (τ). This looks as follows:

$$P = \frac{1}{2}\left(1 - e^{-\left(\frac{\Delta^2 + \delta\tau^2}{2}\right)}\right)$$

(3.2.4)

25

To analyze for correctness, suppose we consider the simple case where there is no difference in frequency, i.e. $\Delta=0$. We then find the experimental signature of the HOM experiment. That is to say that if there is no delay between the photons (i.e. $\delta\tau=0$), then the probability of finding a photon in both photodetectors is 0. If however, as in the classical case, the photons were completely distinguishable, i.e. the difference in frequency was infinite, then this would correspond to a Gaussian distribution, and the probability of detecting a coincidence count would be 50%, as given by the theory.
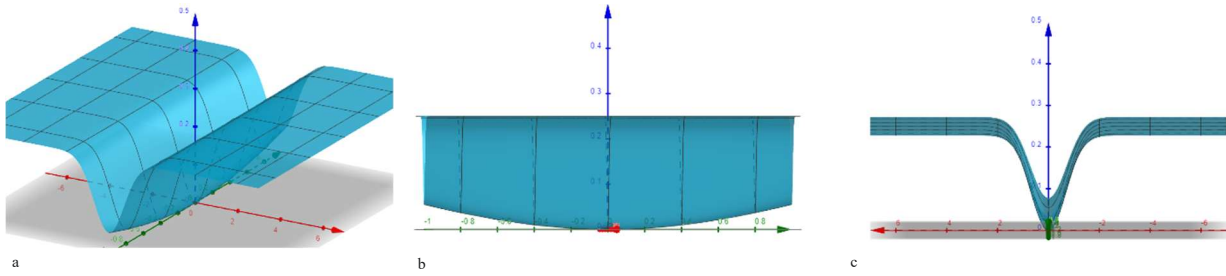

Figure 8 - Probability Distribution for Two Gaussian Photons with a Pulse Width of 2 - Blue axis representing the probability P, the green axis representing frequency difference Δ, and the red axis representing the detection time separation τ. a) Demonstrating the probability distribution with respect to τ and Δ. b) The level curves of probability with respect to frequency difference. c) The level curves of probability with respect to temporal separation

We can graph this distribution as seen in figure 8. The classic HOM dip is present in the graph, but we notice that as the frequency difference between the two photons increases, the dip slowly rises. Therefore there is an increase in the probability of attaining a coincidence count. This rising of the HOM dip would be secondary confirmation of the distinguishability of photons.

~

From the results above, we can confirm that the photons are indeed distinguishable on two fronts, both in the presence of the quantum beat effect in the second-order correlation functions and in the rising of the HOM dip as the frequency increases, suggesting a coincidence count. It is safe to confirm that the HOM experiment can be used to determine the distinguishability of photons in the frequency domain.

CHAPTER 4
CONCLUSIONS AND FUTURE CONSIDERATIONS

A small summary of what has been established thus far: Legero, Wilk, Kuhn, and Rempe (LWKR) provided the mathematical framework for detecting the quantum beat. The presence of this beat serving to suggest that the photons are distinguishable. Given the work done by Woolley, Lang, Eichler, Wallraff, and Blaise, I posited that a similar effect can be observed by mapping the second order correlation functions. Finding the $g^2(t)$ and then integrating it with respect to the detection of the first photon and detection delay between the first and second photons, would then give a probability distribution. Using this probability distribution, it was my hope to find a second mode to verify distinguishability. If the HOM dip were altered, when the frequency was changed, in such a way that suggested there could be a coincidence count; then this would be a confirmed second test for photon distinguishability.

The Gaussian photon of the form given by LWKR is assessed via this framework. However, this required a careful understanding of the temporal mode functions. When quantizing the electromagnetic field, as seen in section 2.1.4.1, it is often done with mode functions that are dependent on polarization. However, this thesis seeks to determine photon distinguishability on the basis of frequency. In order make this consideration, Glauber and Titulær understood that a photons lifetime is closely related to its spatial distribution. As such the mode functions could be written with respect to frequency instead. With this understanding, we now had a mathematical representation for a photon that included frequency.

A HOM experiment was performed on two of these Gaussian photons, wherein two photons are incident upon the beam splitter. From the original experiment, with two photons that are completely indistinguishable, it was found that there were no coincidence counts, i.e. counts where the output photons are incident on the separate detectors. Therefore, it could be considered

that any difference in the frequency of the two photons would be demonstrably different compared to the HOM dip of perfectly indistinguishable photons.

In order to demonstrate this HOM-like dip and the quantum beat effect there needed to be a way to determine the interference between the output photons. We can do this by taking note of the HBT experiment and the second order correlation function. Calculating the $g^2(t)$ of the output photons, and graphing it, would be a visual confirmation for the quantum beat. Not only this, but it could be integrated over detection times to find a probability distribution that could be contrasted with the HOM dip. We are met with the difficulty of not having the exact forms of the output photons. However, this could be bypassed due to the unitary transformation (equation 2.2.2) that describes the action of the beam splitter on the input photons to get the output photons. We are able to attain $g^2(t)$, with respect to the incident photons instead.

Graphing this $g^2(t)$, we were able to find the quantum beat. This was demonstrated by mapping two different frequency differences contrasted against a graph with no frequency difference. As the frequency difference increase, so too did the number of peaks within the envelope, like a beat effect.

Finally the second mode of determining distinguishability, the probability distribution. This was found by integrating the second order correlation function to see if there was a chance for a coincidence count. The integration was performed over all possible first detection times (t) and detection delay times (τ), successfully establishing a distribution of all possible detections. It was found that as the frequency difference increased, the HOM dip steadily rose from zero, suggesting that the probability was no longer 0 to get a coincidence count. This provided second mode of confirmation that the distinguishability of photons could be measured via the HOM effect.

Where do we go from here? Now that I have established a test for determining the distinguishability of photons, it is my intent to put it to use in the PHYS 437 B project. Spontaneous parametric down conversion (SPDC) has been the industry standard for generating entangled photon pairs. However, it is not an on-demand source; and there are now competing producers in the industry, particularly the quantum dot, that seek to take the place of SPDC. I seek to use the results from this thesis to test the quantum dots of the Dr. Reimer's group and determine the distinguishability of the output photons.

~

ACKNOWLEDGEMENTS

I would like to thank everyone who advised, guided, and provided me with the resources to develop and write this thesis. I would first like to thank Dr. Michael Reimer, for his kind and knowledgeable supervision and guidance. I came into this program not knowing how to read research papers and can safely say that it is a skill that I am starting to develop. I would like to thank the members of the Quantum Photonics Devices group for allowing me to attend their group meetings and even contribute by presenting results from research papers. Your informative discussion helped me develop a better understanding of the field. In particular, I'd like to thank Sonell Malik and Matteo Pennacchietti for their tireless help and in helping find relevant resources for my thesis.

I'd also like to thank my family and friends for their unyielding support, I could not have completed this research without you. In particular, my loving husband, who has repeatedly picked me up when I felt as though I was not good enough. My parents, Jayaratnam and Chandrika, for their warm support of my pursuit of knowledge. To Kai who relentlessly tutored me throughout my undergraduate career, whose knowledge I greatly benefitted from. And finally Meagan and Nicole, I would not be anywhere near where I am without you.

Finally, I would like to acknowledge that I completed my research on the promised territory of the Haudenosaunee, Anishinaabe, and Attawandaron peoples. The University of Waterloo is situated on the Haldimand Tract, the land promised to the Six Nations that includes ten kilometers on either side of the Grand River.

BIBLIOGRAPHY

1. Fox, M. (2006). *Quantum Optics An Introduction.* Oxford University Press.

2. Garrow, T. (2021). *Resonant Excitation of a Nanowire Quantum Dot and Optical Frequency Shifting via Electro-Optic Modulation.* Waterloo.

3. Glauber, R. J., & Titualær, U. M. (1966). Density Operators for Coherent Fields. *Physical Review*, 1041-1050.

4. Hong, C. K., Ou, Z. Y., & Mandel, L. (1987). Measurement of Subpicosecond Time Intervals between Two Photons by Interference. *Physical Review Letters*, 2044-2046.

5. Kok, P. (2008).

6. Legero, T., Wilk, T., Kuhn, A., & Rempe, G. (2003). Time-Resolved Two-Photon Quantum Interference. *Applied Physics B*, 797-802.

7. Lundeen, J. S. (n.d.). Retrieved 2022

8. Majidy, S., Laflamme, R., & Wilson, C. (2021). *An Introduction to Building Quantum Computers.*

9. Nave, C. R. (n.d.). *Simple Harmonic Motion* . Retrieved from Hyperphysics: http://hyperphysics.phy-astr.gsu.edu/hbase/shm2.html

10. Omar, Y. (2005). Indistinguishable Particles in Quantum Mechanics: An Introduction. *Contemporary Physics*, 437-438.

11. qutools. (n.d.). *Sample Experiments – 2-Photon-Interference by Hong, Ou & Mandel.* Retrieved from qutools: https://qutools.com/qued/qued-sample-experiments/sample-experiments-hong-ou-mandel/

12. Walmsley, M. G., & Raymer, I. A. (2020). Temporal Modes in Quantum Optics Then and Now. *Physica Scripta*.

13. Woolley, M. J., Lang, C., Eichler, C., Wallraff, A., & Blais, A. (2013). Signatures of Hong–Ou–Mandel Interference at Microwave Frequencies. *New Journal of Physics*.

14. Zhai, L., Nguyen, G. N., Spinnler, C., Ritzmann, J., Löbl, M. C., Wiek, A. D., . . . Warburton, R. J. (2022). Quantum Interference of Identical Photons from Remote GaAs Quantum Dots. *Nature Nanotechnology*.